J Mol Model (2012) 18:4649–4655
DOI 10.1007/s00894-012-1418-z

ORIGINAL PAPER

Theoretical study of structure, bonding, and electronic behavior of novel sandwich compounds $M_3(C_6R_6)_2$ (M = Ni, Pd, Pt; R = H, F)

Ke Zhou

Received: 30 October 2011 / Accepted: 26 March 2012 / Published online: 31 May 2012

Abstract The correlations between the structural and electronic properties of the monolayer clusters M_3 (where M = Ni, Pd, Pt) and the sandwich complexes $M_3(C_6R_6)_2$ (where M = Ni, Pd, Pt; R = H, F) were studied by performing quantum-chemical calculations. All of the sandwich complexes are strongly donating and backdonating metal–ligand bonding structures. The influence of the ligand as well as significant variations in the M–C, M–M, and C–C bond lengths and binding energies were examined to obtain a qualitative and quantitative picture of the intramolecular interactions in C_6R_6–M_3. Our theoretical investigations show that the binding energies of these sandwich complexes gradually decrease from Ni to Pt as well as from H to F, which can be explained via the frontier orbitals of the clusters M_3 and C_6R_6.

Keywords Sandwich complexes · Quantum-chemical calculations · Binding energies

Introduction

The chemistry of metal sandwich complexes has developed intensively since the structure of ferrocene $(C_5H_5)_2Fe$ was first elucidated in 1952 [1, 2]. Metallocenes not only introduced new bonding characteristics of fundamental importance to the field of organometallic chemistry, but have also been utilized in many crucial applications, such as in catalysis, magnetic and optical materials, polymers, molecular recognition, medicine, and nanodevices [3, 4]. Most sandwich complexes possess a mononuclear metal center between two small aromatic carbocyclic ligands, such as cyclopentadienyl or benzene. Among such species, linearly multidecked one-dimensional sandwich complexes have attracted significant interest. $V_n(\text{benzene})_{n+1}$, which have been studied experimentally and theoretically, are expected to serve as nanomagnetic building blocks in applications such as high-density information storage and quantum computing in the future [5–9]. $Li_n(C_6H_6)_{n+1}$ and $Li^+C_6H_6$ complexes yielded good results when used in a model system for graphite/carbon anodes in lithium-ion cells [10]. Moreover, recent density functional theory (DFT) computations suggested that $M_n(\text{ferrocene})_{n+1}$ (M=Sc, Ti, V, Mn) sandwich clusters and nanowires ($n=\infty$) have tunable magnetic properties [11], while $[FeC_5(CH_3)_5]_n$ ($n=\infty$) yields half-metallic sandwich molecular wires with negative differential resistance and sign-reversible high spin-filter efficiency [12]. In addition, bisbenzene dipalladium complexes have been isolated and characterized [13, 14].

Compounds in which the carbon rings flank a monolayer of multiple metal atoms are, however, even more fascinating to chemists. For instance, $Ni_3(\text{benzene})_2$ was detected via mass spectroscopy among a mixture of $Ni_n(\text{benzene})_m$ clusters generated in the gas phase by laser vaporization [15]. Stable structures of discrete metal monolayer sandwich compounds have also been discussed in theoretical studies [16]. Palladium is one of the most versatile transition metal catalysts for transforming organic and inorganic substrates. More recently, two metal monolayer sandwich compounds, $[Pd_3(C_7H_7)_3Cl_3][PPh_4]$ and $[Pd_5(\text{naphthacene})_2(\text{toluene})][B(Ar_f)_4]_2$ (4-toluene), where $B(Ar_f)_4 = B[3,5\text{-}(CF_3)_2C_6H_3]_4$, were synthesized and theoretically analyzed by Tetsuro

K. Zhou (✉)
College of Chemistry and Environmental Science, Shaanxi University of Technology,
723000 Hanzhong, China
e-mail: zhoukejv2_000@yahoo.com.cn

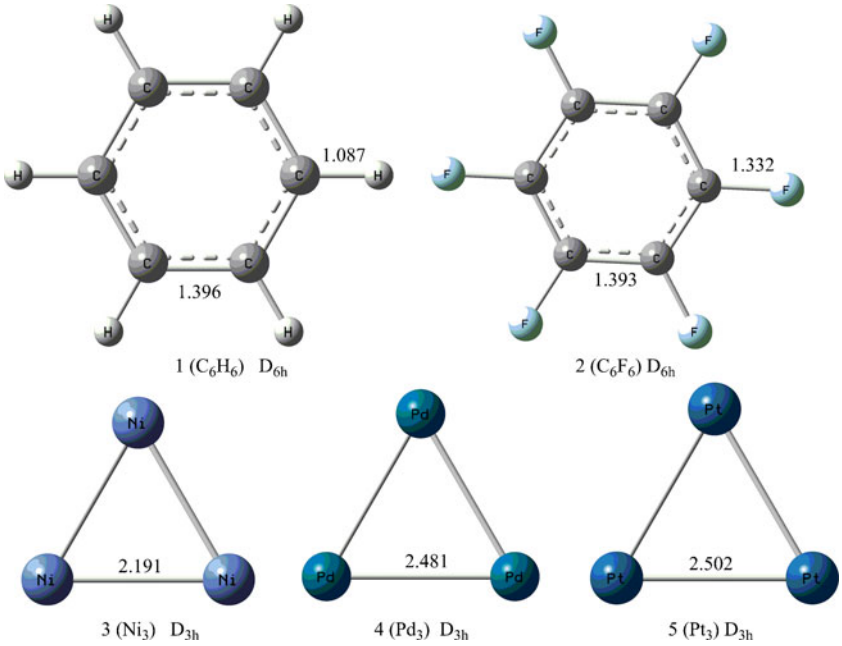

Fig. 1 Structures of the optimized M_3 (M = Ni, Pd, Pt) clusters, C_6H_6, and C_6F_6. The bond lengths shown are in Å

Murahashi and coworkers [17]. The structurally analogous complexes $[Pd_3Tr_2X_2]_\infty$ (X = Cl, Br, and I) and $[Pd_3(C_7H_7)_2X_3]^-$ (X = Cl^-, Br^-, and I^-) were also synthesized and characterized, and calculations were performed on them [18, 19]. Stephanie Hurst found that the palladium–pnictogen bond length in $[Pd_3Tr_2(E)_3][BF_4]_2$ (E = PPh_3, $AsPh_3$, $SbPh_3$, or PEt_3) increases in the order P < As < Sb [20]. Tetsuro Murahashi and coworkers reported an unprecedented square metal sheet sandwich complex $[Pd_4(\mu_4\text{-}C_9H_9)(\mu_4\text{-}C_8H_8)][B(Ar_f)_4]$, where $B(Ar_f)_4$ = B[3,5-$(CF_3)_2(C_6H_3)$]$_4$, in which

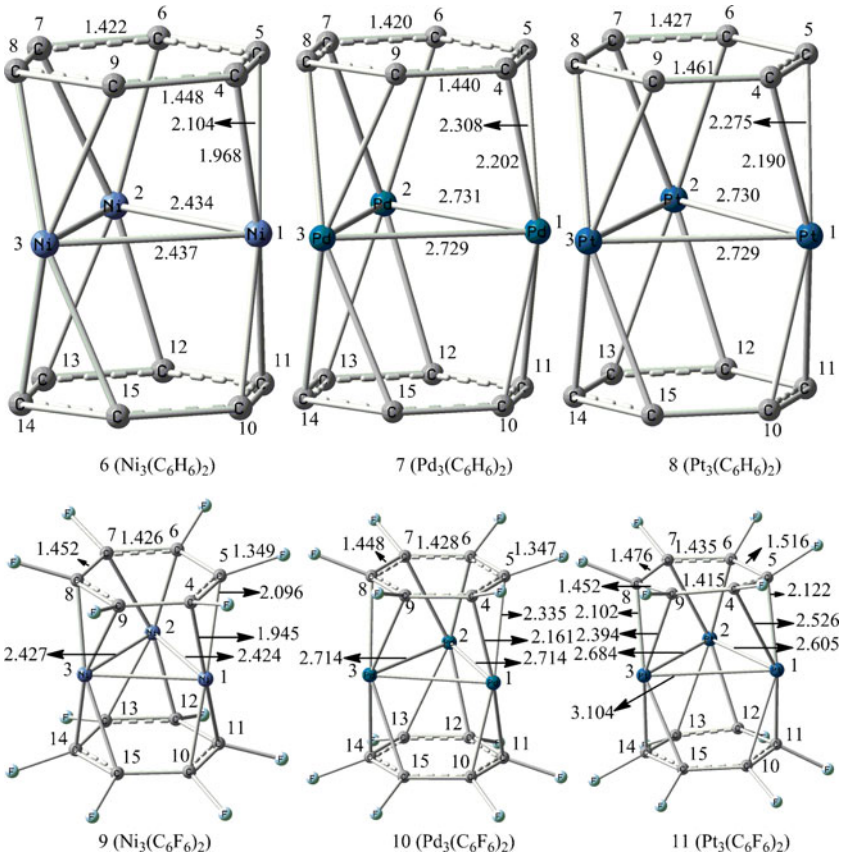

Fig. 2 Structures and atom numbering schemes for the optimized $M_3(C_6R_6)_2$ (M = Ni, Pd, Pt; R = H, F) sandwich structures. The bond lengths shown are in Å. For simplicity and clarity, the H atoms have been omitted

Table 1 Charge populations based on natural atomic orbital occupancies

		s	p_x	p_y	p_z	d_{xy}	d_{xz}	d_{yz}	$d_{x^2-y^2}$	d_{z^2}	d_{total}
Ni_3	Ni1	2.719	2.035	2.025	2.004	1.806	1.997	1.999	1.434	1.981	9.217
	Ni2	2.719	2.035	2.025	2.005	1.806	1.997	1.999	1.434	1.981	9.217
	Ni3	2.719	2.021	2.040	2.005	1.248	1.999	1.999	1.992	1.981	9.219
$Ni_3(C_6H_6)_2$	Ni1	2.234	2.075	2.138	2.097	1.980	1.979	1.690	1.978	1.594	9.221
	Ni2	2.234	2.135	2.079	2.097	1.982	1.757	1.912	1.975	1.594	9.220
	Ni3	2.234	2.110	2.103	2.097	1.974	1.768	1.901	1.983	1.594	9.220
$Ni_3(C_6F_6)_2$	Ni1	2.268	2.132	2.096	2.120	1.973	1.697	1.943	1.971	1.657	9.241
	Ni2	2.268	2.091	2.136	2.120	1.980	1.906	1.733	1.964	1.657	9.240
	Ni3	2.268	2.119	2.109	2.120	1.963	1.855	1.783	1.980	1.658	9.239
Pd_3	Pd1	2.656	2.007	2.041	2.004	1.306	1.999	1.997	1.993	1.997	9.292
	Pd2	2.656	2.033	2.016	2.004	1.821	1.997	1.999	1.478	1.997	9.292
	Pd3	2.656	2.033	2.016	2.004	1.821	1.997	1.999	1.478	1.997	9.292
$Pd_3(C_6H_6)_2$	Pd1	2.222	2.070	2.114	2.069	1.751	1.989	1.991	1.806	1.884	9.421
	Pd2	2.221	2.070	2.087	2.095	1.916	1.825	1.984	1.763	1.934	9.422
	Pd3	2.222	2.070	2.072	2.110	1.943	1.797	1.988	1.760	1.934	9.422
$Pd_3(C_6F_6)_2$	Pd1	2.239	2.089	2.079	2.108	1.936	1.771	1.991	1.755	1.931	9.384
	Pd2	2.239	2.089	2.102	2.085	1.763	1.945	1.984	1.801	1.892	9.385
	Pd3	2.239	2.089	2.100	2.087	1.862	1.844	1.978	1.777	1.923	9.384
Pt_3	Pt1	2.734	2.033	2.020	2.007	1.800	1.996	1.998	1.436	1.977	9.207
	Pt2	2.734	2.033	2.020	2.007	1.800	1.996	1.998	1.435	1.977	9.206
	Pt3	2.734	2.014	2.040	2.007	1.253	1.999	1.995	1.983	1.977	9.207
$Pt_3(C_6H_6)_2$	Pt1	2.364	2.104	2.125	2.084	1.973	1.843	1.815	1.978	1.604	9.213
	Pt2	2.364	2.093	2.137	2.084	1.974	1.955	1.704	1.977	1.603	9.213
	Pt3	2.363	2.147	2.082	2.084	1.979	1.690	1.969	1.972	1.604	9.214
$Pt_3(C_6F_6)_2$	Pt1	2.459	2.104	2.152	2.086	1.691	1.937	1.969	1.716	1.794	9.107
	Pt2	2.482	2.094	2.091	2.078	1.840	1.759	1.947	1.721	1.863	9.130
	Pt3	2.734	2.033	2.020	2.007	1.800	1.996	1.998	1.436	1.977	9.207

cyclononatetraenyl acts as a stable π-coordinating ligand [21]. The aromaticity of this complex was evaluated using NICS indices and the electron localization function, using the AdNDP method, and using NICS and NICSzz indices [22–26]. Recently, Guo and Li presented theoretical results showing that a carbon atom can be incorporated into the M_4 square-planar building block in $[M_4(\mu_4\text{-}C_9H_9)(\mu_4\text{-}C_8H_8)]^+$ (M = Ni, Pd, and Pt) to form the complexes $[M_4C(\mu_4\text{-}C_9H_9)(\mu_4\text{-}C_8H_8)]^+$ (M = Ni, Pd, and Pt) [24–26]. Inspired by these pioneering works, many other similar complexes were subsequently realized experimentally or investigated theoretically [27–32].

In this paper, we report a quantum chemical study of the geometries, binding energies, and bonding

Table 2 Net charge populations[a] on C and M atoms as well as Wiberg indices[b] for structures **1–11**

	Net charge population			Wiberg index					
	M1	C4	C5	M1–M2	M1–M3	M2–M3	M1–C4	M1–C5	C4–C5
6	0.24	−0.34	−0.32	0.22 (0.96)	0.22(0.96)	0.22(0.96)	0.34	0.26	1.31(1.44)
7	0.10	−0.32	−0.30	0.20 (0.93)	0.20(0.93)	0.20 (0.93)	0.26	0.21	1.33
8	0.11	−0.34	−0.30	0.28 (0.97)	0.29(0.97)	0.28 (0.97)	0.35	0.30	1.30
9	0.15	0.25	0.28	0.20	0.22	0.20	0.36	0.28	1.21(1.35)
10	0.10	0.25	0.30	0.18	0.18	0.18	0.29	0.23	1.23
11	0.09	0.35	0.18	0.29	0.19	0.26	0.45	0.32	1.20

[a] Net charge: M1=M2=M3; C4=C6=C8=C10=C12=C14; C5=C7=C9=C11=C13=C15 in structures **6–10**; in structure **11**: 0.09, 0.12, 0.13 for Ni1, Ni2, Ni3, respectively; 0.35, 0.34, 0.29 for C4, C7, C9 respectively; 0.18, 0.27, 0.20, for C5, C6, C8, respectively. [b] The Wiberg indices for C_6H_6, C_6F_6, and the monolayer clusters M_3 are shown in parentheses

Table 3 NICS(0) values of structures **6–11**

	C_6R_6	M_3	M1–C4=C5
6 ($Ni_3(C_6H_6)_2$)	−6.4	−30.4	−48.5
7 ($Pd_3(C_6H_6)_2$)	−7.0	−30.3	−41.9
8 ($Pt_3(C_6H_6)_2$)	−3.0	−30.7	−41.6
9 ($Ni_3(C_6F_6)_2$)	−17.8	−38.5	−44.0
10 ($Pd_3(C_6F_6)_2$)	−16.4	−31.1	−35.1
11 ($Pt_3(C_6F_6)_2$)	−14.0	−34.5	−39.6

characteristics of $M_3(C_6R_6)_2$ (where M = Ni, Pd, Pt; R = H, F) sandwich compounds. In particular, the effects of varying R and M were explored, with several goals. One was to predict further synthetic strategies for them (via donor–acceptor properties, etc.), while another was to get information that can aid our understanding of their structures and enhance the qualitative and quantitative description of their bonding modes and electronic ligand effects.

Computational details

We carried out geometry optimization and frequency evaluation for all of these molecules at the B3PW91 (Becke three-parameter hybrid exchange with Perdew–Wang 1991 gradient corrected correlation) nonlocal density functional [33, 34] level of theory for several states with different multiplicities, $M = 2S + 1$ (S is the total spin). The relativistic effective core potential (RECP) basis set SDD [35] was employed for Ni, Pd, and Pt, and analytical gradients with a polarized split-valence double-ξ, augmented with a diffuse function basis set [6–31+G(d)] were used for other atoms. Vibrational frequency analyses confirmed that each structure was a minimum without an imaginary frequency. The atomic charges were computed via natural population analysis (NPA). Wiberg indices were evaluated and used as bond strength indicators. NBO analysis was performed with NBO version 3.1 [36, 37], which is incorporated into Gaussian 09. Nucleus-independent chemical shifts (NICS, in ppm) [38, 39] were computed using the gauge-independent atomic orbital (GIAO) method [40] at the same level. All of the calculations were performed with the Gaussian 09 program [41].

Results and discussion

Molecular structures

All of the sandwich structures were fully optimized and verified to be local minima without imaginary frequencies (using the B3PW91 computational method) in their low-spin states (M=1), with no symmetry constraints. High-spin states (M=3) were also examined for each of these low-spin structures, but were found to be substantially higher in energy and thus were not considered further.

The structures of the ligands (C_6H_6, C_6F_6) and metal M_3 clusters are presented in Fig. 1. The sandwich structures of $M_3(C_6R_6)_2$ (M = Ni, Pd, Pt; R = H, F) are presented in Fig. 2.

The ligands C_6H_6 and C_6F_6 belong to the D_{6h} point group. The C=C bond length for C_6H_6 is slightly shorter than that for C_6F_6. The central M_3 metal clusters are regular triangle monolayer sheets with D_{3h} symmetry.

The sandwich structures are M_3 metal clusters between two benzene ligands. The benzene rings present an eclipsed geometry, and both rings deviate slightly from planarity. The sandwich structures do not show very high symmetry, which is perhaps due to unbalanced intramolecular torsion. If 0.1 Å is toleranced, they are not D_{3h} but C_{3h} point groups, except for structure **11** (C_1 symmetry). The conjugation normally associated with benzene rings is broken; the C=C distances vary from 1.427 to 1.461 Å for $Pt_3(C_6H_6)_2$, for instance. The central metal M is η^2-coordinated to the C=C bonds of the upper and lower cycloheptatrienyl ligands, respectively. Interestingly, two M–C distances are observed. The distances M1–C4, M1–C10, M2–C6, M2–C12, M3–C8, and M3–C14 are the same, as are the distances M1–C5, M1–C11, M2–C7, M2–C13, M3–C9, and M3–C15. The former set of bonds are always shorter than those of the latter set. All of the intermetallic distances (Ni–Ni, 2.4 Å; Pd–Pd, 2.7 Å; Pt–Pt, 2.6 Å) are within the normal range for M–M single bonds, and are shorter than the corresponding sum of the van der Waals radii (see Fig. 2).

Charge distribution

The nature of the bonding in the sandwich complexes was analyzed at the B3PW91/6-31+G(d)/SDD level from two perspectives: the binding between the metals in the M_3 sheet itself and the interaction between the ligands and the metal sheet.

Table 1 shows that the s and p orbital populations for each metal atom in each sandwich complex and monolayer cluster M_3 are all larger than 2.0 e. In the monolayer clusters, the d_{xy} and $d_{x^2-y^2}$ orbital populations are smaller than 2.0 e, which indicates that d_{xy} and $d_{x^2-y^2}$ contribute to d–d bonding. However, some of the d_{xz}, d_{yz}, and d_z^2 orbital populations are clearly smaller than 2.0 e in the sandwich complexes, which indicates that the d_{xz}, d_{yz}, and d_z^2 orbitals participate in the interaction between the metal monolayer cluster and C_6R_6 (R = H, F). This interaction can be interpreted via donation and backdonation. Taking structure **6**

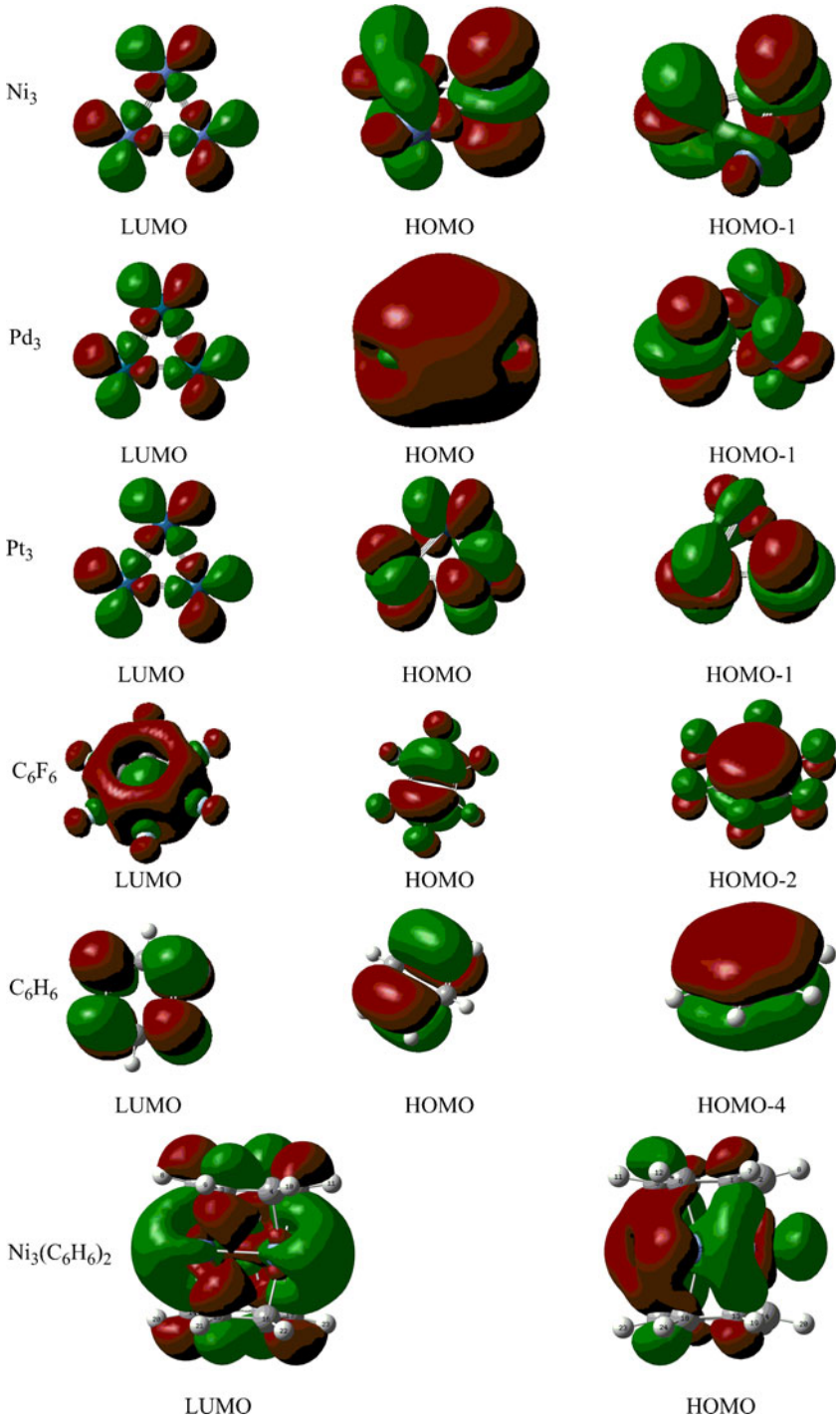

Fig. 3 Frontier orbitals of M_3 (M = Ni, Pd, Pt), C_6R_6 (R = H, F), and $Ni_3(C_6H_6)_2$. The frontier orbitals of the other sandwich compounds are similar to those of $Ni_3(C_6H_6)_2$, so they have been omitted

$[Pd_3(C_6H_6)_2]$ as an example, the natural population analysis (NPA)-calculated charges on the peripheral C4, C5, and Ni1 atoms are −0.34, −0.32, and +0.24, respectively. Note that the carbon acts as a charge acceptor, and that this compensates for the donation by the carbon. The atomic electron configurations are $[He]2s^{0.96}2p_x^{1.17}2p_y^{1.10}2p_z^{1.08}$ for the C4 atom and $[He]2s^{0.96}2p_x^{1.18}2p_y^{1.09}2p_z^{1.07}$ for the C5 atom. The relatively high $2p_x$ and $2p_y$ occupancies and lower occupancies for the $2p_z$ orbitals are manifestations of the backdonation from C to M.

In structures **6**, **7**, and **8**, M has a net positive charge, while carbon has a net negative charge. The charges on C(4, 6, 8, 10, 12, 14) are higher than those on C(5, 7, 9, 11, 13, 15), which indicates that the bonds between M and C(4, 6, 8, 10, 12, 14) are shorter. In **9**, **10**, and **11**, all of the carbons have a net positive charge, because fluorine is an electron acceptor. The charges

on C(4, 6, 8, 10, 12, 14) are lower than those on C(5, 7, 9, 11, 13, 15), which explains why the bonds between M and C(4, 6, 8, 10, 12, 14) are shorter—there is greater electrostatic repulsion for these bonds.

Wiberg indices were evaluated and used as bond strength indicators (see Table 2). The WBIs for M–M change enormously upon the formation of sandwich complexes [from 0.93–0.97 for M_3 to 0.18–0.29 for $M_3(C_6R_6)_2$, respectively], which agrees with the changes in M–M and C–C bond lengths observed. There are two values for the M–C Wiberg index, which is consistent with the two different M–C bond lengths. Also, the M–M WBIs in the sandwich complexes imply slightly stronger interactions between the Ni atoms and Pt atoms than in the Pd_3 sheet.

Aromaticity

NICS can be used to predict and understand some of the properties of a molecule, especially its stability due to aromatic stabilization, which is based on the negative of the magnetic shielding computed at or above the geometrical centers of rings or clusters. Systems with negative NICS values are aromatic. We computed the NICS(0) values at the geometric centers of all of the rings (C_6H_6, C_6F_6, M_3, M1–C4=C5). The NICS values computed at the B3PW91/6-31+G(d)/SDD level of theory are listed in Table 3. Evidently, the NICS values at the M_3 and M1–C4=C5 triangle ring centers are all highly negative (M_3: −38.5 to 30.3; M1–C4=C5: −35.1 to −48.5), suggesting a high degree of aromaticity and stability. In contrast, the NICS values of the C_6R_6 rings are small (−17.8 to −3.0). The aromaticity can also be determined via the frontier orbitals (see Fig. 3).

Binding energy and stability

The binding energy was also studied at the B3PW91/SDD/6-311+G(d) level of theory. The binding energies ΔE for these neutral complexes are defined as:

$$\Delta E = \{E[M_3(C_6R_6)_2])\} - \{E[M_3] + 2E[C_6R_6]\}. \quad (1)$$

The binding energies ΔE (see Table 4) for these neutral complexes include zero-point contributions. Basis set superposition error (BSSE) corrections were carried out using the counterpoise method [42]. ΔE_B represents the binding energy corrected for the BSSE. The Gibbs free energies ΔG are also presented in Table 4 in order to judge whether can gain the sandwich complexes. All of the binding energies and Gibbs free energies are negative, which indicates that the sandwich complexes are stable. The binding energies of the sandwich complexes gradually decrease from Ni to Pt, as well as from H to F, which shows that Ni_3(benzene)$_2$ is the most stable, as expected based on experimental data. $Pt_3(C_6F_6)_2$ is the most difficult species to synthesize.

Table 4 Binding energies (kJ mol^{-1}), Gibbs free energies (kJ mol^{-1}), and HOMO–LUMO gap energies (ΔE_g, eV) of the sandwich complexes

	ΔE	ΔE_B	ΔG	ΔE_g
6 $[Ni_3(C_6H_6)_2]$	−413.06	−383.06	−295.56	2.72
7 $[Pd_3(C_6H_6)_2]$	−358.84	−342.63	−241.86	2.99
8 $[Pt_3(C_6H_6)_2]$	−301.40	−280.19	−182.52	2.72
9 $[Ni_3(C_6F_6)_2]$	−288.45	−239.56	−170.11	2.99
10 $[Pd_3(C_6F_6)_2]$	−178.29	−156.80	−61.36	3.26
11 $[Pt_3(C_6F_6)_2]$	−125.48	−89.44	−3.3291	2.08

All energies are in kJ mol^{-1}; ΔE and ΔE_B represent the binding energy without and with BSSE correction, respectively. ΔG represents the Gibbs free energy at 298 K

The variations in the binding energies can also be interpreted using the frontier orbitals in Fig. 3. The HOMO of Ni_3 is a bonding (π) orbital, with the dominant contributions arising from the d_{z^2}, $d_{x^2-y^2}$, and d_{xy} orbitals of the central Ni atom. The HOMO of Pd_3 is an extensively delocalized σ orbital that mainly consists of contributions from the s and d_{z^2} orbitals. Although the delocalization of the HOMO of Pd_3 is more extensive than that of Ni_3, the HOMO is mainly delocalized at the center of Pd_3, so this greater delocalization does not lead to greater molecular orbital overlap between C_6R_6 and Pd_3; indeed, the binding energy of $Pd_3(C_6R_6)_2$ is less than that of $Ni_3(C_6R_6)_2$. The HOMO of Pt_3 is an antibonding orbital that receives contributions from the s and d_z^2 orbitals, so the binding energy of $Pt_3(C_6R_6)_2$ is lower than those of $Pd_3(C_6R_6)_2$ and $Ni_3(C_6R_6)_2$. On the other hand, this may be interpreted as being due to the increasing effect of the inert electron pair from Ni to Pt. The HOMO and HOMO-2 of C_6F_6 are delocalized over not only the carbon ring but also the F atoms, while the HOMO and HOMO-2 of C_6H_6 are only delocalized over the carbon ring. Therefore, the electron density in the carbon ring of C_6H_6 is greater, and the binding energies of the sandwich complexes gradually reduce from H to F. In the end, all of the sandwich complexes exhibit HOMO–LUMO gap energies of >2.08 eV (see Table 4), implying that they are all relatively kinetically stable.

Conclusions

In summary, we computationally designed six new members of the sandwich complex family, each of which consists of C_6H_6 or C_6F_6 ligands with a Ni_3, Pd_3, or Pt_3 monolayer sheet between them. The bonding between the C_6H_6 or C_6F_6

ligands and the M_3 monolayer sheet can be interpreted as electron donation from the C_6R_6 rings to the M_3 and back-donation from the latter to the former. NICS calculations show that the M_3 monolayer sheet is strongly aromatic, as is each M1–C=C triangle ring, which yields insight into the stability of sandwich compounds. Furthermore, the binding energies of the sandwich complexes gradually decrease from Ni to Pt, as well as from H to F. We hope that this study will stimulate future experimental efforts aimed at realizing new nanomaterials based on such sandwich structures.

Acknowledgments I am grateful for the financial support of the Natural Science Basic Research Plan in Shaanxi Province of China (No.2009JM1012).

References

1. Wilkinson G, Rosenblum M, Whiting MC, Woodward B (1952) J Am Chem Soc 74:2125–2126
2. Fischer EO, Pfab W (1952) Naturforsch B 7:377–379
3. Jin P, Li FY, Chen ZF (2011) J Phys Chem A 115:2402–2408
4. Muetterties EL, Bleeke JR, Wucherer EJ, Albright TA (1982) Chem Rev 82:499–525
5. Nagaoka S, Matsumoto T, Ikemoto K, Mitsui M, Nakajima A (2007) J Am Chem Soc 129:1528–1529
6. Kandalam AK, Rao BK, Jena P, Pandey R (2004) J Chem Phys 120:10414–10422
7. Wang J, Acioli PH, Jellinek J (2005) J Am Chem Soc 127:2812–2813
8. Wang J, Jellinek J (2005) J Phys Chem A 109:10180–10182
9. Xiang HJ, Yang JL, Hou JG, Zhu QS (2006) J Am Chem Soc 128:2310–2314
10. Vollmer JM, Kandalam AK, Curtiss LA (2002) J Phys Chem A 106:9533–9537
11. Zhang X, Wang J, Gao Y, Zeng XC (2009) ACS Nano 3:537–545
12. Wang L, Gao X, Yan X, Zhou J, Gao Z, Nagase S, Sanvito S, Maeda Y, Akasaka T, Mei WN, Lu J (2010) J Phys Chem C 114:21893–21899
13. Allegra G, Immirzi A, Porri L (1965) J Am Chem Soc 87:1394–1395
14. Gorlov M, Fischer A, Kloo L (2004) J Organomet Chem 689:489–492
15. Kurikawa T, Takeda H, Hirano M, Judai K, Arita T, Nagao S, Nakajima A, Kaya K (1999) Organometallics 18:1430–1438
16. Burdett JK, Canadell E (1985) Organometallics 4:805–815
17. Murahashi T, Fujimoto M, Oka M, Hashimoto Y, Uemura T, Tatsumi Y, Nakao Y, Ikeda A, Sakaki S, Kurosawa H (2006) Science 313:1104–1107
18. Mulligan FL, Babbini DC, Davis IR, Hurst SK, Nichol GS (2009) Inorg Chem 48:2708–2710
19. Muñoz-Castro A, Arratia-Pérez R (2010) J Phys Chem A 114:5217–5221
20. Babbini DC, Mulligan FL, Schulhauser HR, Sweigart TC, Nichol GS, Hurst SK (2010) Inorg Chem 49:4307–4312
21. Murahashi T, Inoue R, Usui K, Ogoshi S (2009) J Am Chem Soc 131:9888–9889
22. Muñoz-Castro A, Carey DM-L, Arratia-Pérez R (2010) J Chem Phys 132:164308–164314
23. Sergeeva AP, Boldyrev AI (2010) Phys Chem Chem Phys 12:12050–12054
24. Guo JC, Li SD (2010) Eur J Inorg Chem 32:5156–5160
25. Tsipis AC, Kefalidis CE, Tsipis CA (2008) J Am Chem Soc 130:9144–9155
26. Galeev TR, Boldyrev AI (2011) Annu Rep Prog Chem Sect C107:124–147
27. Tatsumi Y, Shirato K, Murahashi T, Ogoshi S, Kurosawa H (2006) Angew Chem Int Ed 45:5799–5803
28. Murahashi T, Kato N, Uemura T, Kurosawa H (2007) Angew Chem Int Ed 46:3509–3512
29. Murahashi T, Fujimoto M, Kawabata Y, Inoue R, Ogoshi S, Kurosawa H (2007) Angew Chem Int Ed 46:5440–5443
30. Murahashi T, Hashimoto Y, Chiyoda K, Fujimoto M, Uemura T, Inoue R, Ogoshi S, Kurosawa H (2008) J Am Chem Soc 130:8586–8587
31. Muñiz J, Sansores LE, Martínez A, Salcedo R (2008) J Mol Model 14:427–434
32. Valencia I, Castro M (2010) J Phys Chem A 114:21–28
33. Becke AD (1993) J Chem Phys 98:5648–5652
34. Perdew JP, Wang Y (1992) Phys Rev B 45:13244–13249
35. Schwerdtfeger P, Dolg M, Schwarz WHE, Bowmaker GA, Boyd PDW (1989) J Chem Phys 91:1762–1774
36. Glendening ED, Reed AE, Carpenter JE, Weinhold F (2001) NBO program, version 3.1. University of Wisconsin, Madison
37. Reed AE, Curtiss LA, Weinhold F (1988) Chem Rev 88:899–926
38. Schleyer PvR, Maerker C, Dransfeld A, Jiao H, Hommes NJRvE (1996) J Am Chem Soc 118:6317–6318
39. Chen ZF, Wannere CS, Corminboeuf C, Puchta R, Schleyer PvR (2005) Chem Rev 105:3842–3888
40. Wolinski K, Hilton JF, Pulay P (1990) J Am Chem Soc 112:8251–8260
41. Frisch MJ, Trucks GW, Schlegel HB, Scuseria GE, Robb MA, Cheeseman JR, Scalmani G, Barone V, Mennucci B, Petersson GA, Nakatsuji H, Caricato M, Li X, Hratchian HP, Izmaylov AF, Bloino J, Zheng G, Sonnenberg JL, Hada M, Ehara M, Toyota K, Fukuda R, Hasegawa J, Ishida M, Nakajima T, Honda Y, Kitao O, Nakai H, Vreven T, Montgomery JA Jr, Peralta JE, Ogliaro F, Bearpark M, Heyd JJ, Brothers E, Kudin KN, Staroverov VN, Kobayashi R, Normand J, Raghavachari K, Rendell A, Burant JC, Iyengar SS, Tomasi J, Cossi M, Rega N, Millam JM, Klene M, Knox JE, Cross JB, Bakken V, Adamo C, Jaramillo J, Gomperts R, Stratmann RE, Yazyev O, Austin AJ, Cammi R, Pomelli C, Ochterski JW, Martin RL, Morokuma K, Zakrzewski VG, Voth GA, Salvador P, Dannenberg JJ, Dapprich S, Daniels AD, Farkas O, Foresman JB, Ortiz JV, Cioslowski J, Fox DJ (2009) Gaussian 09, revision A.02.Smp. Gaussian Inc., Wallingford
42. Boys SF, Bernardi F (1970) Mol Phys 19:553–566